

Microbial Control of Sea Spray Aerosol Composition: A Tale of Two Blooms

Xiaofei Wang,^{†,‡} Camille M. Sultana,^{†,‡} Jonathan Trueblood,[§] Thomas C. J. Hill,^{||} Francesca Malfatti,^{⊥,#} Christopher Lee,[†] Olga Laskina,[§] Kathryn A. Moore,[†] Charlotte M. Beall,[⊥] Christina S. McCluskey,^{||} Gavin C. Cornwell,[†] Yanyan Zhou,^{⊥,▽} Joshua L. Cox,[†] Matthew A. Pendergraft,[⊥] Mitchell V. Santander,[†] Timothy H. Bertram,^{||} Christopher D. Cappa,[§] Farooq Azam,[⊥] Paul J. DeMott,^{||} Vicki H. Grassian,[§] and Kimberly A. Prather^{*,†,⊥}

[†]Department of Chemistry and Biochemistry, University of California, San Diego, La Jolla, California 92093, United States

[§]Department of Chemistry, University of Iowa, Iowa City, Iowa 52242, United States

^{||}Department of Atmospheric Science, Colorado State University, Fort Collins, Colorado 80523, United States

[⊥]Scripps Institution of Oceanography, University of California, San Diego, La Jolla, California 92093, United States

[#]National Institute of Oceanography and Experimental Geophysics, Trieste 34100, Italy

[▽]State Key Laboratory of Marine Environmental Science and Key Laboratory of the MOE for Coastal and Wetland Ecosystems, School of Life Sciences, Xiamen University, Xiamen 361005, P. R. China

^{||}Department of Chemistry, University of Wisconsin—Madison, Madison, Wisconsin 53706, United States

[§]Department of Civil and Environmental Engineering, University of California, Davis, Davis, California 95616, United States

Supporting Information

ABSTRACT: With the oceans covering 71% of the Earth, sea spray aerosol (SSA) particles profoundly impact climate through their ability to scatter solar radiation and serve as seeds for cloud formation. The climate properties can change when sea salt particles become mixed with insoluble organic material formed in ocean regions with phytoplankton blooms. Currently, the extent to which SSA chemical composition and climate properties are altered by biological processes in the ocean is uncertain. To better understand the factors controlling SSA composition, we carried out a mesocosm study in an isolated ocean-atmosphere facility containing 3,400 gallons of natural seawater. Over the course of the study, two successive phytoplankton blooms resulted in SSA with vastly different composition and properties. During the first bloom, aliphatic-rich organics were enhanced in submicron SSA and tracked the abundance of phytoplankton as indicated by chlorophyll-a concentrations. In contrast, the second bloom showed no enhancement of organic species in submicron particles. A concurrent increase in ice nucleating SSA particles was also observed only during the first bloom. Analysis of the temporal variability in the concentration of aliphatic-rich organic species, using a kinetic model, suggests that the observed enhancement in SSA organic content is set by a delicate balance between the rate of phytoplankton primary production of labile lipids and enzymatic induced degradation. This study establishes a mechanistic framework indicating that biological processes in the ocean and SSA chemical composition are coupled not simply by ocean chlorophyll-a concentrations, but are modulated by microbial degradation processes. This work provides unique insight into the biological, chemical, and physical processes that control SSA chemical composition, that when properly accounted for may explain the observed differences in SSA composition between field studies.



INTRODUCTION

Sea spray aerosols (SSA) represent a major atmospheric aerosol particle type.^{1–3} SSA play a crucial role in affecting climate through reducing direct radiative forcing⁴ and by modulating cloud properties through their ability to act as cloud condensation nuclei⁵ and ice nucleating particles (INP).⁶ Estimates of the impact of SSA on the Earth's radiation budget are highly uncertain due to an overall lack of understanding of

the physical and chemical factors controlling SSA concentration, size, and composition.^{5,7–9} This limits our ability to untangle the extent to which human activities versus the natural background have altered the impacts of particles on the global radiation budget and climate, and thus hampers assessments of

Received: April 14, 2015

Published: May 18, 2015

future climate change.¹⁰ Freshly emitted SSA are composed of both sea salt and organic material, and under certain conditions the organic species comprise a substantial fraction of the total particle mass, especially for smaller diameter particles (<1 μm).^{11,12} The lower solubility organic components can strongly affect the climate-relevant properties of SSA.^{13–15} However, due to a limited understanding of the mechanisms that control the transfer of organic matter from seawater to SSA, it is currently not possible to predict the organic composition of SSA.

Ideally, the organic content of SSA could be predicted using some measured seawater chemical or biological parameter. Significant effort has been put into developing relationships between the organic fraction of SSA and chlorophyll-a (Chl-a) concentrations, an indicator of seawater phytoplankton concentrations, because Chl-a in surface waters can be measured from space using satellites.¹⁶ Results from previous studies have been ambiguous. Some field studies have shown a relationship between the organic fraction of SSA and Chl-a concentrations for monthly and seasonal time scales in ambient marine aerosols,^{12,17} while others have reported no differences in sea spray composition.^{15,18} Further, the coefficient of determination (r^2) between Chl-a and organic fraction in SSA is usually below 0.5.¹⁹ This suggests that the organic enrichment of SSA is controlled not only by phytoplankton primary production but also by other biological and chemical processes. Nevertheless, Chl-a is still commonly used to estimate the organic fraction of SSA in large-scale climate models.^{5,20,21} Thus, if sea spray composition and the associated properties are to be properly treated in models, it is crucial to elucidate the mechanisms that link oceanic biological activity, surface ocean chemical composition and concentrations, and the organic fraction of SSA.

Herein new insights into these mechanistic linkages have been achieved through the use of a unique ocean-atmosphere facility¹³ that allows for detailed characterization of seawater and the associated SSA produced from wave breaking during a 29-day mesocosm experiment utilizing real ocean water. Using a kinetic model, we have established a mechanistic explanation tying the control of seawater organic composition by the measured biological metrics of chlorophyll-a and heterotrophic bacteria enzyme activity to submicron SSA organic concentration and composition. The results from this study provide a possible explanation for the conflicting results in field studies investigating the factors controlling the organic content of SSA and the associated climate properties.

RESULTS AND DISCUSSION

Overview of Mesocosm Experiment and Measurements. A mesocosm experiment was performed in a wave channel filled with 3,400 gallons of natural seawater obtained off the California coast. This unique ocean-atmosphere facility allowed for simulation of ocean seawater conditions representative of typical oceanic phytoplankton blooms with respect to the Chl-a concentrations.²² Dynamic oceanic chemical processes associated with biological activity were stimulated by addition of nutrients at the beginning of the experiment, which initiated phytoplankton growth (Methods S1–S4). Two successive, yet distinct, phytoplankton blooms resulted as evidenced by two major Chl-a peaks over the 29-day experimental period (Figure 1A). Seawater biological activity was characterized by measurements of Chl-a and heterotrophic bacteria concentrations and ectoenzyme activities (Method S5).

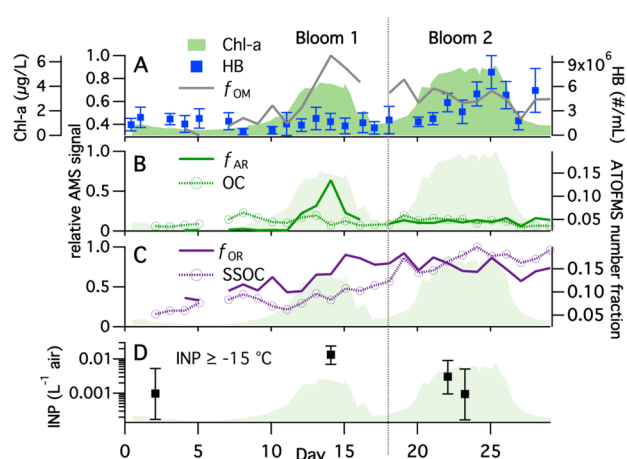


Figure 1. Time series for the mesocosm experiment in the wave channel of (A) Chl-a and heterotrophic bacteria (HB) concentrations in bulk seawater and as f_{OM} , the relative organic mass fraction of SSA as determined by the AMS; (B) f_{AR} , the relative aliphatic-rich factor mass fraction and the number fraction of the OC particle type; (C) f_{OR} , the relative oxygen-rich factor mass fraction and the number fraction of the SSOC particle type as determined by the AMS and ATOFMS respectively; and (D) the concentration of ice nucleating particles (INP).

Throughout this entire study, realistic nascent SSA were generated from the seawater using actual breaking waves⁵ (Figure S1) and the SSA size distributions and composition, both bulk and size-resolved, were measured (Methods S6–S9). Size-resolved bulk chemical composition of nonrefractory SSA components (in particular, organic matter, OM) of dry particles in the size range 0.04 to 2 μm (vacuum aerodynamic diameter, D_{va}) was measured online using an Aerodyne high-resolution time-of-flight aerosol mass spectrometer (AMS; Method S7). The normalized OM mass fraction of SSA, f_{OM} , was determined as $f_{\text{OM}} = [\text{OM}]/[\text{PM}_{1.0}]_{\text{dry}}$, normalized to the maximum value of f_{OM} , where $[\text{PM}_{1.0}]_{\text{dry}}$ is the dry submicron particulate mass concentration estimated from the size distributions (Method S8). The chemical compositions of dried individual SSA particles from 0.25 to 3 μm (D_{va}) were additionally characterized online using an aerosol time-of-flight mass spectrometer (ATOFMS), which measures the size-resolved chemical mixing state of particles and allows for determination of variations in the relative fractions and concentrations of particles with distinct compositions (Method S7). These online measurements were complemented by offline measurements of individual particle organic composition using micro-Raman spectroscopy (Method S9).

Impact of Mesocosm Dynamics on SSA Composition. The behavior of the f_{OM} time series was distinct between the two phytoplankton blooms; f_{OM} peaked during the first bloom, then decreased and remained constant throughout the second bloom (Figure 1A). The variability in f_{OM} suggests a difference in the organic composition of the seawater between the two blooms, examined further below, and helps to explain why previous studies have found inconsistent correlations between organic enrichment in SSA and phytoplankton blooms or Chl-a concentrations in seawater.^{12,15,18,21} Further insights come from consideration of the average size distribution of AMS organic species ion signals (Figure 2A). The peaks at m/z 43, 57, and 44 are used as indicators of total, aliphatic-rich, and oxidized organic species, respectively.²³ The study-average total organic

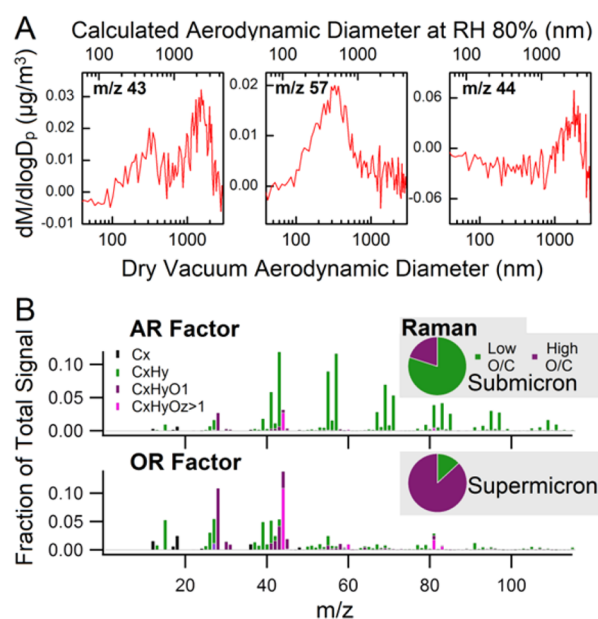


Figure 2. Two organic size modes in SSA produced from the wave-channel experiment. (A) Mass size distributions of AMS organic ion signals: m/z 43 ($C_3H_7^+$ or $C_2H_3O^+$), an indicator of total organic species; m/z 57 ($C_4H_9^+$), an indicator of aliphatic-rich organic species; and m/z 44 (CO_2^+), an indicator of oxidized organic species. The AMS measured particle size as dry D_{va} and the aerodynamic diameter (D_a) at RH 80% was calculated (Method S8) and shown on the top x -axis. (B) AMS mass spectra of the two organic component factors, aliphatic-rich and oxygen-rich, which were separated by positive matrix factorization (PMF); and (inset) classification of submicron (D_a : 0.56–1 μm) and supermicron (D_a : 1.8–3.2 μm) particles based on micro-Raman spectra of individual SSA particles collected on day 14. The data shown accounts for 94% and 81% respectively of all the submicron and supermicron particles analyzed on day 14.

size distribution was bimodal, with clear chemical differences between the classes of organic compounds in these two modes. The submicron mode peaked at $D_{va} = 300$ nm and was dominated by aliphatic-rich organic species, whereas the supermicron mode peaked at $D_{va} = 1500$ nm and was dominated by oxidized organic species, consistent with the size-resolved mass spectra (Figure S2).

SSA are formed when bubbles burst at the air–sea interface, producing both film drops and jet drops.² Film drops are formed from the bursting of the bubble film, which is enriched in surface active organic species,²⁴ while jet drops may originate from the sea surface microlayer (SSML) or underlying bulk seawater. These differences in production mechanisms can lead to differences in the resulting SSA composition. It is typically assumed that most submicron SSA originate from film drops, while most supermicron SSA originate from jet drops.^{24,25} Aliphatic-rich organic species, such as lipids, are typically surface active, allowing them to partition strongly to bubble surfaces and the air–sea interface. This can lead to organic enrichment in film drops, especially if bubble drainage of water occurs,²⁶ although there can be a complex relationship between enrichment in the SSML and the bulk concentrations of surface active species.^{27,28} In contrast, the more oxidized organic species in the supermicron mode were chemically similar to the dissolved organics in the seawater, as evidenced by comparison with the AMS organic spectrum of atomized bulk seawater (Figure S3). Given the differences in the size and composition of the two organic modes of SSA, we postulate that the

aliphatic-rich submicron mode particles were mainly generated from film drops, while jet drops contributed to the supermicron mode particles that contained the more soluble oxidized organic compounds. It should be noted that this is the first time the production mechanism has been shown to distribute different classes of organic species to different size modes.

The AMS organic signals were separated into two factor components using positive matrix factorization (Method S8, Figure 2B), and the oxygen-to-carbon (O/C) and hydrogen-to-carbon (H/C) atomic ratios of the total organic matter were extracted through analysis of the high-resolution mass spectra. The mass spectrum for one of the factors was dominated by hydrocarbon peaks ($C_xH_y^+$), similar to that of the organics in the submicron mode (Figure S3); this factor will be referred to as the aliphatic-rich (AR) factor. The mass spectrum for the second factor was similar to the average supermicron mode organic mass spectrum (Figure S3) and contained many oxygen-containing organic peaks ($C_xH_yO_z^+$); this factor will be referred to as the oxygen-rich (OR) factor. Thus, the AR and OR factors are representative of the organic species comprising the submicron and supermicron modes, respectively.

Figure 1B,C shows the time series of the AR and OR factor mass concentrations, normalized to $[PM_{10}]_{dry}$ and the maximum value of f_{OM} , referred to as f_{AR} and f_{OR} (Method S8). Both f_{AR} (Figure 1B) and the H/C ratio of the total organic matter (Figure S4) exhibited a sharp peak during the first phytoplankton bloom, quickly declined, and then remained nearly constant throughout the second bloom. The sudden decrease in the f_{AR} peak was nearly concurrent with the decline of the Chl-*a* concentrations in the first bloom, suggesting that the submicron mode became enriched in labile organic species that underwent rapid transformations through microbial activity in the seawater. The observation that f_{AR} peaked only during one of the blooms indicates that there were clear differences in the production and degradation of the organic species that made up most of the submicron organic mass. The half-life of these labile species was <1 day, as f_{AR} decreased by more than 50% within 1 day of the peak. Known labile species in seawater include amino acids, proteins, free sugars, fatty acids, and other lipids.^{29,30} The AR factor was rich in aliphatic character, and thus lipids seem a more likely source of the submicron organics than do proteins or free sugars. The f_{OR} time series exhibited distinctly different behavior from that of f_{AR} , increasing from the onset of the first bloom, after which it remained relatively constant (Figure 1C), suggesting that the more oxidized organic species in the supermicron mode had comparably much longer residence times in seawater than AR species. These findings demonstrate that organic species in seawater cannot be considered a homogeneous pool in terms of how they influence organic enrichment in SSA, and that biological degradation processes coupled with differences in the production mechanism lead to partitioning of distinct classes of organic species into separate SSA size modes at different times during a phytoplankton bloom.

The general organic types (aliphatic-rich and oxygen-rich) are further supported by offline measurements using micro-Raman spectroscopy of individual, substrate-deposited particles in different size ranges (Method S9). During the peak of the first bloom (day 14), submicron particles (aerodynamic diameter D_a : 0.56–1 μm) were dominated by compounds having low O/C ratios (O/C < 0.25), while supermicron particles (D_a : 1.8–3.2 μm) contained mostly compounds having a high O/C ratio (O/C > 0.5) (Figure 2B). The O/C

ratio of individual particles was estimated from the molecular formulas of representative compounds (Figure S6). Thus, the micro-Raman results further support the mass spectrometry results showing different classes of organic species contributing to particles in the two SSA size modes.

Analysis of the ATOFMS mass spectra led to identification of two distinct organic-enriched SSA particle types (Method S7): sea salt mixed with organic carbon species (SSOC) and organic carbon species largely free of sea salt (OC) (Figure S5A), both of which are similar to previously described particle types.¹³ Whereas the AMS allowed for characterization of the bulk organic composition, the ATOFMS characterizes individual particle types, making these two online mass spectrometry approaches complementary. Supermicron particles (1–3 μm) were dominated by the SSOC type, with SSOC particles 2 to 3 times more abundant than OC type particles in this size range. Further, the time series of the total SSOC number fraction was similar to that of f_{OR} (Figure 1C), which suggests a relationship between oxygen-rich species and SSOC type particles. The relative number fraction of the OC particle type increased steeply with decreasing size, making up a greater fraction of total particles than SSOC in the smallest size bin (0.25–0.5 μm). This indicates a connection between OC type particles and the AR organics in the submicron mode, although the time series of the total OC number fraction was fairly constant over time, in contrast to the sharp peak in f_{AR} (Figure 1B). However, the total OC number fraction time series is not necessarily representative of the behavior of particles with dry $D_{\text{va}} < 0.5 \mu\text{m}$, which make up <1% of the total particle counts due to the size-dependent sampling bias of the ATOFMS (Figure S5B). The particle sampling statistics do not lend themselves to a presentation of the time series in the relevant submicron size range (dry $D_{\text{va}} \sim 0.3 \mu\text{m}$). Based on the combined AMS and ATOFMS results, the aliphatic-rich organic species in the submicron particles most likely occur in particles largely free of sodium chloride (i.e., OC type) while the oxygen-rich organic species in the supermicron mode were more likely to be internally mixed with sea salt (i.e., SSOC type).

Explaining the Differences in SSA Organic Content between the Two Blooms. The second phytoplankton bloom in the wave channel did not lead to organic enrichment in the submicron mode, suggesting that some process other than phytoplankton primary production must have played a role in controlling the abundance and chemical composition of organic material transferred to submicron SSA. Heterotrophic bacteria (HB) concentrations (Figure 1A) and enzymatic activity as characterized by the lipase activity (Figure 3) were much higher during the second bloom than during the first, and both exhibited similar temporal variations. It is therefore possible that primary production by phytoplankton introduced surface-active, aliphatic-rich, highly labile (ARL) organic species to the seawater that led to the sharp increase in f_{AR} (i.e., in aliphatic-rich organics in submicron SSA) during the first bloom. However, this buildup in ARL species—and thus in f_{AR} —was halted and reversed as the HB concentration and enzymatic activity increased, leading to an increased rate of transformation of ARL species into less surface active, more soluble species. Although these degradation products likely remained in the seawater,³¹ they were transferred less efficiently into submicron SSA by film drops thereby causing f_{AR} to decrease and remain low throughout the second bloom. It is likely that the more soluble degradation products, likely fatty acid salts, contributed to organics species in the supermicron

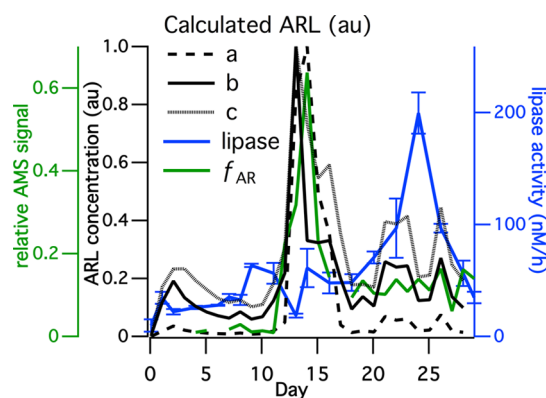


Figure 3. Lipase activity and calculated aliphatic-rich labile (ARL) species concentration. Model parameters: (a) $k^+ = 250 \text{ au } \mu\text{g}^{-1} \text{ L day}^{-1}$ and $C_{1/2} = 30 \text{ au}$; (b) $k^+ = 6 \text{ au } \mu\text{g}^{-1} \text{ L day}^{-1}$ and $C_{1/2} = 5 \text{ au}$; and (c) $k^+ = 6 \text{ au } \mu\text{g}^{-1} \text{ L day}^{-1}$ and $C_{1/2} = 500 \text{ au}$ (au means arbitrary unit).

mode which began to increase after the first bloom. The most likely identity of the ARL organic species was lipids such as glyceroglycolipids, phospholipids, and triacylglycerols, which make up the majority of lipids produced by phytoplankton in seawater.^{32,33} Fatty acids are less likely to be the ARL organic species because they are generally more soluble and less surface active than other lipids classes and lack ester bonds.³⁴ Additionally, the turnover time for free fatty acids in the ocean is around 10 days,^{25,26} much longer than the 1 day observed in the first bloom. Consistent with the above ideas, it is well established that heterotrophic bacteria in seawater use ectoenzymatic lipase to transform ester-containing lipids by hydrolysis into smaller molecular weight and comparably more soluble free fatty acids or their salts.²⁹ Thus, we suggest that the sharp decrease in f_{AR} at the end of the first bloom and the sustained low level throughout the second bloom resulted from the increase in heterotrophic bacteria concentrations and the associated lipase enzymatic activity.

This hypothesis is quantitatively examined using a box model in which it is assumed that ARL species are produced by phytoplankton and transformed by bacteria via lipase (Method S11). More specifically, ARL production is assumed to correlate with the death and disruption (cell lysis) of the phytoplankton, which usually results from programmed cell death or virus or zooplankton attack, which serves as a major source of dissolved organic matter (DOM) in seawater.^{26,35} In this study, zooplankton likely do not play an important role since most zooplankton were removed by filtering at the start of the experiment (Method S2). Additionally viral lysis of phytoplankton was excluded from the model because the observed virus concentration correlated with the HB concentration ($r^2 = 0.60$), indicating that most of the viruses in the mesocosm experiment, which were at typical ocean concentrations,³⁶ were likely bacteriophages that do not attack phytoplankton.^{37,38} Therefore, for this mesocosm experiment, programmed cell death is thought to control phytoplankton cell lysis, and the production rate of ARL was assumed to be first order and proportional to the Chl-a (and phytoplankton mass) concentrations. The transformation rate of the ARL species was assumed to follow Michaelis–Menten kinetics.²⁹ Thus, the model is governed by the following equation:

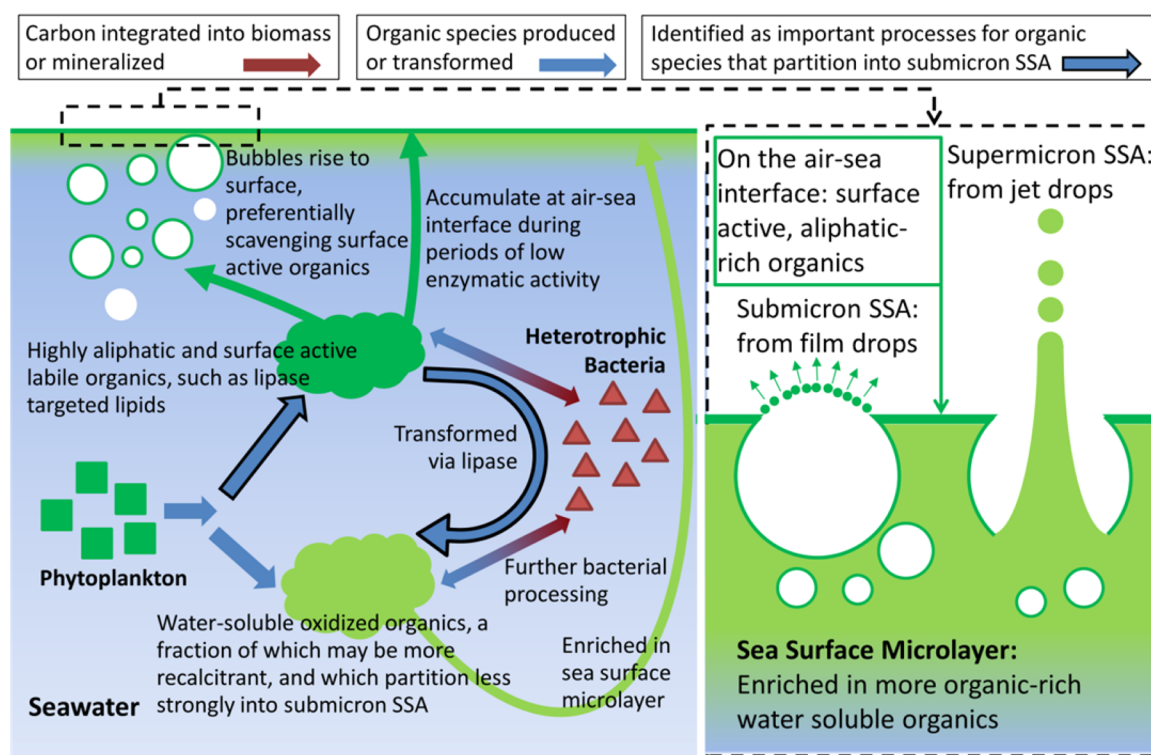


Figure 4. Schematic for the pathways of organic enrichment in SSA and their possible relationships with biological processes in seawater.

$$\frac{d[\text{ARL}]}{dt} = k^+[\text{Chl-a}] - R_{\max}[\text{ARL}]/(C_{1/2} + [\text{ARL}]) \quad (1)$$

where k^+ is the ARL production rate constant and $C_{1/2}$ is the ARL concentration at half of its maximum consumption rate, both of which are adjustable parameters. The observed [Chl-a] time series is used as a model input. The parameter R_{\max} is the maximum transformation rate of ARL, which is related to the enzymatic activity. Here, R_{\max} is assumed to be equal to the measured time series of lipase activity.

The model parameters have been adjusted to determine an [ARL] time series that reproduces the shape of the f_{AR} time series (Figure 3). This comparison implicitly assumes that variations in [ARL] are linearly related to f_{AR} , which is reasonable if the surface-active ARL species are below the surface saturation threshold; this assumption may break down at high ARL concentrations.^{27,28} This model shows good agreement between the calculated [ARL] and the observed f_{AR} after tuning (Figure 3), which strongly supports our hypothesis that enzymatic degradation, driven by bacterial lipases, led to the rapid reduction in f_{AR} after the first bloom and the sustained low concentrations during the second bloom. Ectoenzyme activities besides lipase, including protease, chitinase, and alkaline phosphatase, were also measured. However, these ectoenzyme activities showed very different temporal trends from lipase (Figure S7), and no values of the adjustable model parameters were found that yielded a good fit to the f_{AR} time series when these were used either individually or summed together. This further supports the idea that bacterial lipase activity was specifically responsible for the degradation of ARL species. Thus, bacterial enzymes are responsible for converting insoluble lipids into more soluble free fatty acids as the primary ARL transformation pathway.^{32,33} The change in solubility induced by the enzymes results in different classes of organic

species being released in different SSA size modes, as described above.

The above model excludes processes resulting from cell lysis of heterotrophic bacteria which could be a source of mostly phospholipids, rather than triacylglycerols and glyceroglycolipids,^{39,40} although it is unlikely that contributions from bacteria cell lysis would compete globally with primary lipid production from phytoplankton.²⁶ Also of consideration is the level of lipase activity during the blooms, which was $\sim 50 \text{ nM h}^{-1}$ during the first bloom with a peak of 200 nM h^{-1} during the second bloom. Unpublished measurements of lipase activity of the natural seawater at the SIO pier range from 8 to 30 nM h^{-1} . Lower values have been observed in more oligotrophic sites,⁴¹ while similarly high values have been observed in the northern Adriatic Sea⁴² and in other mesocosm experiments.⁴³ The implication of having high lipase activity, relative to oceanic blooms, is that the ARL transformation may have proceeded more rapidly during the mesocosm experiment, thus limiting the duration of the submicron SSA organic enrichment.

Taking all the results together, the contribution of organics to the submicron SSA mode (here, exemplified by f_{AR}) is determined by the combined effects of the production and transformation of key surface-active species. Thus, the use of Chl-a as an indicator of organic enrichment in submicron SSA consequently only provides one piece of the story. Based on our findings, we recommend that future studies include measurements of bacterial enzyme activities to provide a more complete picture of the production and formation pathways for organic species in seawater to explain submicron SSA composition.

Impact of Phytoplankton Bloom on Ice Nucleation Properties. As SSA particles influence clouds and represent the dominant particle type available to serve as cloud nucleating particles in remote marine environments,^{4,44} variations in SSA

chemical composition induced by biological activity have been suggested to lead to the observed changes in cloud properties in these regions.¹³ Here we investigate how concentrations of ice nucleating particles (INP) changed during the mesocosm experiment through SSA collection and release into liquid for immersion freezing studies in solution (Method S10). The observed INP concentrations ($0.001\text{--}0.014\text{ L}^{-1}$ at $-15\text{ }^{\circ}\text{C}$) were similar to those observed in remote ($>45^{\circ}\text{S}$) marine air.³² The maximum warm-temperature INP concentration (i.e., ice nucleation at $\geq -15\text{ }^{\circ}\text{C}$) occurred concurrent with the peak in f_{AR} during the first bloom (Figure 1D). The INP activity during this period was reduced from 0.014 L^{-1} to below the detection limit for this sample by preheating the solution to $95\text{ }^{\circ}\text{C}$, suggesting that biological particles were released concurrently with the AR organics in SSA. Additionally, monolayers of surface-active long-chain molecules could also have triggered ice nucleation on SSA; for example, amphiphilic long-chain alcohol monolayers have been shown to trigger heterogeneous freezing of water.^{45,46} It is important to note that the INP which appear to be biological particles based on the heat treatment results could have been released concurrently with the change in SSA composition of submicron particles. Although the exact species that led to the increased INP concentrations during the first bloom are not yet confirmed, the observation that the INP concentration peaked during a phytoplankton bloom suggests that changes in the chemical composition and complexity of seawater, induced by biological processes, can influence the release of ice nucleating particles, a finding which has significant implications for marine cloud properties and global climate.

Factors Controlling SSA Composition and Climate-Relevant Properties. A mechanistic overview of the major findings of this mesocosm experiment is provided in Figure 4. Chemically distinct pools of different organic compounds are proposed to exist in seawater. Differences in chemical composition between these pools determine both their biological availability and transfer to the aerosol phase, leading to clear distinctions in organic speciation and mixing state of organic-containing submicron and supermicron SSA. As evident from the mesocosm experiment here, these separate organic pools were transferred to SSA at different times and in different particle size ranges over the course of two successive phytoplankton blooms.

During the first bloom only, aliphatic-rich organic species in SSA peaked sharply and generally tracked Chl-a concentrations. The AR organics were primarily in submicron particles with little, if any, contribution from NaCl, indicating that they were most likely generated primarily from the bursting of the bubble film cap as purely organic particles. A similar mechanism was proposed recently based on the observation that the organic fraction of artificially generated sea spray from natural waters in the field was more aliphatic-rich from areas of higher Chl-a concentrations.⁴⁷ Increased concentrations of ice nucleating particles were associated with the increase of these aliphatic-rich organic species, thus illustrating the potential climatic impacts of variations in SSA chemical composition. However, no enrichment in AR organics occurred during the second bloom despite higher peak Chl-a concentrations. It is proposed here that the AR organics are phytoplankton-produced, surface-active, labile organic species, such as ester-containing lipids, that are subject to hydrolysis by enzymatic activity of bacterial lipase. This mechanism is supported by a kinetic box model that was constrained by measured Chl-a concentrations and

lipase activity and that associates variations in calculated seawater labile AR organics with variations in the observed AR organics in submicron SSA for the two phytoplankton blooms in the wave channel. In contrast, the supermicron mode SSA organics were identified as being comparably oxygen-rich and likely mixed with sea salt. These OR organics are likely more soluble than the AR organics and less surface active, and it is proposed that the OR organics are transferred to SSA primarily via jet drop production. The organic precursors contributing to the supermicron SSA are likely relatively more recalcitrant in nature and products of either phytoplankton primary production, bacteria degradation, or secondary production, making their temporal behavior difficult to model. Future mesocosm studies should focus on obtaining a more complete understanding of the factors contributing to the fate of these OR organic species in seawater.

A recent study¹² detected no difference in the amount of organic enrichment in SSA in areas of high and low biological activity, leading the authors to conclude that background levels of organic species overwhelm those produced by biological activity in seawater and make up the organic content of SSA. However, the current study demonstrates that biological processes can indeed impact the organic content of SSA. First it is shown here that the organic species contributing to submicron and supermicron SSA are different chemical classes and show different temporal behavior over the course of the bloom. Second, the extent of organic enrichment in submicron SSA particles depends on a competition between phytoplankton production and bacterial degradation of surface-active organic species. This study therefore provides a mechanistic explanation as to why Chl-a has proven to be an inconsistent predictor of organic enrichment in SSA particles. Clearly, predictions of organic enrichment and the resulting impacts on cloud properties in marine environments require additional measurements besides Chl-a levels. Specifically, the history of the phytoplankton bloom, timing of the SSA measurements relative to the bloom life cycle, heterotrophic bacteria concentrations, and the associated level of enzymatic activity also play determinant roles.

■ ASSOCIATED CONTENT

📎 Supporting Information

The following file is available free of charge on the ACS Publications website at DOI: [10.1021/acscentsci.5b00148](https://doi.org/10.1021/acscentsci.5b00148).

Details on the experimental methods, a detailed description of the model, and additional figures (PDF)

■ AUTHOR INFORMATION

Corresponding Author

*E-mail: kprather@ucsd.edu. Tel: 1- 858-822-5312.

Author Contributions

‡X.W. and C.M.S. contributed equally.

Notes

The authors declare no competing financial interest.

■ ACKNOWLEDGMENTS

This material is based upon work supported by the National Science Foundation through the Centers of Chemical Innovation Program under Grant CHE1305427. We would like to thank Paul Harvey and the entire staff of the Scripps Institution of Oceanography Hydraulics Laboratory for facilitating use of the laboratory and technical support in

maintaining the wave channel. We would also like to thank Susannah Burrows, Douglas Collins, Luisa Galgani, Renee Williams, and Richard Cochran for many helpful discussions.

REFERENCES

(1) O'Dowd, C. D.; De Leeuw, G. Marine aerosol production: a review of the current knowledge. *Philos. Trans. R. Soc., A* **2007**, *365*, 1753–1774.

(2) Lewis, E. R.; Schwartz, S. E. *Sea Salt Aerosol Production: Mechanisms, Methods, Measurements and Models—A Critical Review*; American Geophysical Union: Washington, DC, 2004.

(3) Stier, P.; Feichter, J.; Roeckner, E.; Kloster, S.; Esch, M. The evolution of the global aerosol system in a transient climate simulation from 1860 to 2100. *Atmos. Chem. Phys.* **2006**, *6*, 3059–3076.

(4) Murphy, D. M.; Anderson, J. R.; Quinn, P. K.; McInnes, L. M.; Brechtel, F. J.; Kreidenweis, S. M.; Middlebrook, A. M.; Posfai, M.; Thomson, D. S.; Buseck, P. R. Influence of sea-salt on aerosol radiative properties in the Southern Ocean marine boundary layer. *Nature* **1998**, *392*, 62–65.

(5) Partanen, A. I.; Dunne, E. M.; Bergman, T.; Laakso, A.; Kokkola, H.; Ovadnevaite, J.; Sogacheva, L.; Bainsée, D.; Sciare, J.; Manders, A.; O'Dowd, C.; de Leeuw, G.; Korhonen, H. Global modelling of direct and indirect effects of sea spray aerosol using a source function encapsulating wave state. *Atmos. Chem. Phys.* **2014**, *14*, 11731–11752.

(6) DeMott, P. J.; Prenni, A. J.; Liu, X.; Kreidenweis, S. M.; Petters, M. D.; Twohy, C. H.; Richardson, M. S.; Eidhammer, T.; Rogers, D. C. Predicting global atmospheric ice nuclei distributions and their impacts on climate. *Proc. Natl. Acad. Sci. U.S.A.* **2010**, *107*, 11217–11222.

(7) de Leeuw, G.; Andreas, E. L.; Anguelova, M. D.; Fairall, C. W.; Lewis, E. R.; O'Dowd, C.; Schulz, M.; Schwartz, S. E. Production flux of sea spray aerosol. *Rev. Geophys.* **2011**, *49*, RG2001.

(8) O'Dowd, C. D.; Langmann, B.; Varghese, S.; Scannell, C.; Ceburnis, D.; Facchini, M. C. A combined organic-inorganic sea-spray source function. *Geophys. Res. Lett.* **2008**, *35*, L01801.

(9) Jaeglé, L.; Quinn, P. K.; Bates, T. S.; Alexander, B.; Lin, J. T. Global distribution of sea salt aerosols: new constraints from in situ and remote sensing observations. *Atmos. Chem. Phys.* **2011**, *11*, 3137–3157.

(10) IPCC. *Climate Change 2013: The Physical Science Basis. Contribution of Working Group I to the Fifth Assessment Report of the Intergovernmental Panel on Climate Change*; Cambridge University Press: Cambridge, U.K., and New York, NY, USA, 2013.

(11) Hoffman, E. J.; Duce, R. A. The organic carbon content of marine aerosols collected on Bermuda. *J. Geophys. Res.: Atmos.* **1974**, *79*, 4474–4477.

(12) O'Dowd, C. D.; Facchini, M. C.; Cavalli, F.; Ceburnis, D.; Mircea, M.; Decesari, S.; Fuzzi, S.; Yoon, Y. J.; Putaud, J. P. Biogenically driven organic contribution to marine aerosol. *Nature* **2004**, *431*, 676–680.

(13) Prather, K. A.; Bertram, T. H.; Grassian, V. H.; Deane, G. B.; Stokes, M. D.; DeMott, P. J.; Aluwihare, L. I.; Palenik, B. P.; Azam, F.; Seinfeld, J. H.; Moffet, R. C.; Molina, M. J.; Cappa, C. D.; Geiger, F. M.; Roberts, G. C.; Russell, L. M.; Ault, A. P.; Baltrusaitis, J.; Collins, D. B.; Corrigan, C. E.; Cuadra-Rodriguez, L. A.; Ebben, C. J.; Forestieri, S. D.; Guasco, T. L.; Hersey, S. P.; Kim, M. J.; Lambert, W. F.; Modini, R. L.; Mui, W.; Pedler, B. E.; Ruppel, M. J.; Ryder, O. S.; Schoepp, N. G.; Sullivan, R. C.; Zhao, D. F. Bringing the ocean into the laboratory to probe the chemical complexity of sea spray aerosol. *Proc. Natl. Acad. Sci. U.S.A.* **2013**, *110*, 7550–7555.

(14) Collins, D. B.; Ault, A. P.; Moffet, R. C.; Ruppel, M. J.; Cuadra-Rodriguez, L. A.; Guasco, T. L.; Corrigan, C. E.; Pedler, B. E.; Azam, F.; Aluwihare, L. I.; Bertram, T. H.; Roberts, G. C.; Grassian, V. H.; Prather, K. A. Impact of marine biogeochemistry on the chemical mixing state and cloud forming ability of nascent sea spray aerosol. *J. Geophys. Res.: Atmos.* **2013**, *118*, 8553–8565.

(15) Quinn, P. K.; Bates, T. S.; Schulz, K. S.; Coffman, D. J.; Frossard, A. A.; Russell, L. M.; Keene, W. C.; Kieber, D. J.

Contribution of sea surface carbon pool to organic matter enrichment in sea spray aerosol. *Nat. Geosci.* **2014**, *7*, 228–232.

(16) McClain, C. R. A Decade of Satellite Ocean Color Observations. *Annu. Rev. Mar. Sci.* **2009**, *1*, 19–42.

(17) Rinaldi, M.; Decesari, S.; Finessi, E.; Giulianelli, L.; Carbone, C.; Fuzzi, S.; O'Dowd, C. D.; Ceburnis, D.; Facchini, M. C. Primary and Secondary Organic Marine Aerosol and Oceanic Biological Activity: Recent Results and New Perspectives for Future Studies. *Adv. Meteorol.* **2010**, *2010*, 310682.

(18) Bates, T. S.; Quinn, P. K.; Frossard, A. A.; Russell, L. M.; Hakala, J.; Petäjä, T.; Kulmala, M.; Covert, D. S.; Cappa, C. D.; Li, S. M.; Hayden, K. L.; Nuaaman, I.; McLaren, R.; Massoli, P.; Canagaratna, M. R.; Onasch, T. B.; Sueper, D.; Worsnop, D. R.; Keene, W. C. Measurements of ocean derived aerosol off the coast of California. *J. Geophys. Res.: Atmos.* **2012**, *117*, D00V15.

(19) Rinaldi, M.; Fuzzi, S.; Decesari, S.; Marullo, S.; Santoleri, R.; Provenzale, A.; von Hardenberg, J.; Ceburnis, D.; Vaishya, A.; O'Dowd, C. D.; Facchini, M. C. Is chlorophyll-a the best surrogate for organic matter enrichment in submicron primary marine aerosol? *J. Geophys. Res.: Atmos.* **2013**, *118*, 4964–4973.

(20) Spracklen, D. V.; Arnold, S. R.; Sciare, J.; Carslaw, K. S.; Pio, C. Globally significant oceanic source of organic carbon aerosol. *Geophys. Res. Lett.* **2008**, *35*, L12811.

(21) Vignati, E.; Facchini, M. C.; Rinaldi, M.; Scannell, C.; Ceburnis, D.; Sciare, J.; Kanakidou, M.; Myriokefalitakis, S.; Dentener, F.; O'Dowd, C. D. Global scale emission and distribution of sea-spray aerosol: Sea-salt and organic enrichment. *Atmos. Environ.* **2010**, *44*, 670–677.

(22) Wernand, M. R.; van der Woerd, H. J.; Gieskes, W. W. C. Trends in Ocean Colour and Chlorophyll Concentration from 1889 to 2000, Worldwide. *PLoS One* **2013**, *8*, e63766.

(23) Canagaratna, M. R.; Jayne, J. T.; Jimenez, J. L.; Allan, J. D.; Alfarra, M. R.; Zhang, Q.; Onasch, T. B.; Drewnick, F.; Coe, H.; Middlebrook, A.; Delia, A.; Williams, L. R.; Trimborn, A. M.; Northway, M. J.; DeCarlo, P. F.; Kolb, C. E.; Davidovits, P.; Worsnop, D. R. Chemical and microphysical characterization of ambient aerosols with the aerodyne aerosol mass spectrometer. *Mass Spectrom. Rev.* **2007**, *26*, 185–222.

(24) Blanchard, D. The ejection of drops from the sea and their enrichment with bacteria and other materials: A review. *Estuaries* **1989**, *12*, 127–137.

(25) Grythe, H.; Ström, J.; Krejci, R.; Quinn, P.; Stohl, A. A review of sea-spray aerosol source functions using a large global set of sea salt aerosol concentration measurements. *Atmos. Chem. Phys.* **2014**, *14*, 1277–1297.

(26) Burrows, S. M.; Ogunro, O.; Frossard, A. A.; Russell, L. M.; Rasch, P. J.; Elliott, S. M. A physically based framework for modeling the organic fractionation of sea spray aerosol from bubble film Langmuir equilibria. *Atmos. Chem. Phys.* **2014**, *14*, 13601–13629.

(27) Marty, J. C.; Žutić, V.; Precali, R.; Saliot, A.; Čosović, B.; Smoldaka, N.; Cauwet, G. Organic matter characterization in the Northern Adriatic sea with special reference to the sea surface microlayer. *Mar. Chem.* **1988**, *25*, 243–263.

(28) Wurl, O.; Wurl, E.; Miller, L.; Johnson, K.; Vagle, S. Formation and global distribution of sea-surface microlayers. *Biogeosciences* **2011**, *8*, 121–135.

(29) Kirchman, D. L. *Microbial Ecology of the Oceans*, 2nd ed.; Wiley-Blackwell: Hoboken, NJ, 2008.

(30) Goutx, M.; Guigue, C.; D, D. A.; Ghiglione, J. F.; Pujol-Pay, M.; Raybaud, V.; Duflos, M.; Prieur, L. Short term summer to autumn variability of dissolved lipid classes in the Ligurian sea (NW Mediterranean). *Biogeosciences* **2009**, *6*, 1229–1246.

(31) Duflos, M.; Goutx, M.; Van Wambeke, F. Determination of Lipid Degradation by Marine Lipase-Producing Bacteria: Critical Evaluation of Lipase Activity Assays. *Lipids* **2009**, *44*, 1113–1124.

(32) Harwood, J. L.; Guschina, I. A. The versatility of algae and their lipid metabolism. *Biochimie* **2009**, *91*, 679–684.

- (33) Gupta, R.; Gupta, N.; Rathi, P. Bacterial lipases: an overview of production, purification and biochemical properties. *Appl. Microbiol. Biotechnol.* **2004**, *64*, 763–781.
- (34) Gašparović, B.; Kozarac, Z.; Saliot, A.; Čosović, B.; Möbius, D. Physicochemical Characterization of Natural and ex-Situ Reconstructed Sea-Surface Microlayers. *J. Colloid Interface Sci.* **1998**, *208*, 191–202.
- (35) Kujawinski, E. B.; Farrington, J. W.; Moffett, J. W. Evidence for grazing-mediated production of dissolved surface-active material by marine protists. *Mar. Chem.* **2002**, *77*, 133–142.
- (36) Breitbart, M. Marine Viruses: Truth or Dare. *Annu. Rev. Mar. Sci.* **2012**, *4*, 425–448.
- (37) Wilcox, R. M.; Fuhrman, J. A. Bacterial viruses in coastal seawater: lytic rather than lysogenic production. *Mar. Ecol.: Prog. Ser.* **1994**, *114*, 35–45.
- (38) Suttle, C. A. Marine viruses—major players in the global ecosystem. *Nat. Rev. Microbiol.* **2007**, *5*, 801–812.
- (39) Van Mooy, B. A. S.; Fredricks, H. F. Bacterial and eukaryotic intact polar lipids in the eastern subtropical South Pacific: Water-column distribution, planktonic sources, and fatty acid composition. *Geochim. Cosmochim. Acta* **2010**, *74*, 6499–6516.
- (40) Kaneda, T. Iso- and anteiso-fatty acids in bacteria: biosynthesis, function, and taxonomic significance. *Microbiol. Rev.* **1991**, *55*, 288–302.
- (41) Bourguet, N.; Torrèton, J.-P.; Galy, O.; Arondel, V.; Goutx, M. Application of a Specific and Sensitive Radiometric Assay for Microbial Lipase Activities in Marine Water Samples from the Lagoon of Nouméa. *Appl. Environ. Microbiol.* **2003**, *69*, 7395–7400.
- (42) Celussi, M.; Del Negro, P. Microbial degradation at a shallow coastal site: Long-term spectra and rates of exoenzymatic activities in the NE Adriatic Sea. *Estuarine, Coastal Shelf Sci.* **2012**, *115*, 75–86.
- (43) Riemann, L.; Steward, G. F.; Azam, F. Dynamics of Bacterial Community Composition and Activity during a Mesocosm Diatom Bloom. *Appl. Environ. Microbiol.* **2000**, *66*, 578–587.
- (44) Burrows, S. M.; Hoose, C.; Pöschl, U.; Lawrence, M. G. Ice nuclei in marine air: biogenic particles or dust? *Atmos. Chem. Phys.* **2013**, *13*, 245–267.
- (45) Gavish, M.; Popovitz-Biro, R.; Lahav, M.; Leiserowitz, L. Ice Nucleation by Alcohols Arranged in Monolayers at the Surface of Water Drops. *Science* **1990**, *250*, 973–975.
- (46) Popovitz-Biro, R.; Gavish, M.; Lahav, M.; Leiserowitz, L. Ice nucleation by monolayers of aliphatic alcohols. *Makromol. Chem., Macromol. Symp.* **1991**, *46*, 125–132.
- (47) Frossard, A. A.; Russell, L. M.; Burrows, S. M.; Elliott, S. M.; Bates, T. S.; Quinn, P. K. Sources and composition of submicron organic mass in marine aerosol particles. *J. Geophys. Res.: Atmos.* **2014**, *119*, 12977–13003.